



## Parametric study of a membrane energy exchanger based on energy, entropy, and exergy analysis for proton exchange membrane fuel cell application

Ebrahim Shahbazi | Nasser Baharlou-Houreh\*  | Karim Maghsoudi | Parsa Zirak

Department of Mechanical Engineering, Shahid Rajaei Teacher Training University, Tehran, Iran

\* Corresponding author, Email: [Nasser.baharloo@sru.ac.ir](mailto:Nasser.baharloo@sru.ac.ir)

### Article Information

#### Article Type

RESEARCH ARTICLE

#### Article History

RECEIVED: 15 Jun 2024

REVISED: 14 Aug 2024

ACCEPTED: 02 Sep 2024

PUBLISHED ONLINE: 05 Sep 2024

#### Keywords

Membrane energy exchanger

Exergy efficiency

Sensitivity analysis

WRR

### Abstract

The present study adopted the thermodynamic technique to model a membrane energy exchanger (MEE) used for proton exchange membrane fuel cell (PEMFC) application. Governing equations, including a system of three nonlinear coupled equations and several dependent equations, are solved. The present numerical results were compared and validated by an experimental study, indicating a suitable match with a reasonable error. A comprehensive parametric study and sensitivity analysis were conducted in this study based on four efficiency evaluation criteria, including effectiveness, water recovery ratio (WRR), entropy generation, and exergy efficiency. The exergy efficiency comprises the thermodynamic exergy, chemical exergy, and mechanical exergy. The analyzed parameters included temperature at the wet and dry channel entry, pressure at the wet and dry channel entry, and relative humidity (RH) at the wet and dry channel entry. A to D ratings were assigned to these parameters. When three criteria show positive results by enhancing each parameter, the A rating is assigned to that parameter, representing the optimal efficiency. For example, enhancing the dry channel entry temperature from 306 to 318 K leads to a 30.5% enhancement in WRR, a decrease in DPAT, an 11% improvement in exergy efficiency, and a reduction in entropy generation. Since all four criteria were desirable, enhancing the dry channel entry temperature was rated A and is highly recommended.

**Cite this article:** Shahbazi, E., Baharlou-Houreh, N., Maghsoudi, K, Zirak, P. (2024). Parametric study of a membrane energy exchanger based on energy, entropy, and exergy analysis for proton exchange membrane fuel cell application. DOI: [10.22104/HFE.2024.6846.1293](https://doi.org/10.22104/HFE.2024.6846.1293)



© The Author(s).

DOI: [10.22104/HFE.2024.6846.1293](https://doi.org/10.22104/HFE.2024.6846.1293)

Publisher: Iranian Research Organization for Science and Technology (IROST)

## 1 Introduction

The increase in energy consumption and global warming due to the emission of greenhouse gases caused by the consumption of fossil fuels is one of the motivating factors in the development of renewable energies, including fuel cells [1,2]. Fuel cells are a kind of chemical energy converter to electrical energy with a great potential to produce electricity and heat [3–5]. In proton exchange membrane fuel cells (PEMFC), humidity of the membrane should be balanced because low humidity causes dryness of the membrane and high humidity leads to the flooding phenomenon, resulting in a decreased efficiency of the PEMFC [6]. The efficiency of a PEMFC is enhanced by about 20 to 40% with proper humidification of reactive gases [7,8]. Controlling the temperature and humidity of gases entering the PEMFC complex is carried out through two methods: Internal and external humidification. In external humidification system, the reactive gases are humidified before entering the PEMFC; however, in the internal humidification system, the cooling and humidification systems are integrated with the PEMFC system. Internal humidification methods include chemical and physical approaches. Bubble humidifiers, enthalpy wheel energy exchanger, membrane energy exchanger (MEE), etc. are among the most used examples of external humidifiers. Accurate and convenient control of the temperature and humidity of gases entering the PEMFC is one of the advantages of external humidification system.

One of the most common external humidification methods is the use of a MEE. MEE is a type of heat and moisture exchanger based on a polymer membrane, which has major applications in building air conditioning systems [9], PEMFCs, water desalinations [10], medicine [11], and chemical reactors [12]. MEEs are in different sizes and have types of membranes depending on their application and the working fluid used. Based on the working fluid, MEEs are divided into two types: air-to-air and liquid-to-air. In terms of geometric shape, MEEs can be classified into plate type (or frame and plate) and tubular type (or shell and tube). The plate type is usually used for air-to-air MEEs and shell-and-tube type is usually employed for liquid-to-air MEEs. According to the fluid flow direction, MEEs are divided into three categories: co, cross and counter flow. Meanwhile, the counter-flow one is the most used one.

Several studies have been conducted on MEE in recent years. Wolfenstetter et al. [13] assessed experimentally the influence of temperature, relative humidity (RH), and pressure on water transfer within three

Nafion membranes 115, 211, and 212 with different thicknesses in an air-to-air plate MEE. In the reference test, a heating furnace was used to ensure isothermal conditions and improve the quality of measurements. A comparison between membrane of Nafion and an ultra-thin membrane of composite showed that the thicker Nafion membrane has less water transfer at upper temperatures, while the moisture transfer in the membrane of composite does not depend on the temperature. Examining co-flow, cross-flow and counter-flow arrangements showed that the type of flow arrangement has little effect on water transfer.

Baharlou Houreh et al. [14] experimentally compared a plate MEE with cross-flow and a plate MEE with co-flow and counter-flow to analyze the effects of flow rate at the wet channel, flow rate at the dry channel and equal flow rate in two channels on MEE efficiency. They performed the experiments for two boundary conditions, insulating and isothermal. The results indicated that water recovery ratio (WRR) increased with the enhance in the dry channel flow rate for all flow arrangements. It was found that in a certain flow rate, the co-flow increases the WRR by 5 to 27% compared to the counter-flow and the cross-flow enhances the WRR by 2 to 10% compared to the co-flow. Park and Jung [15] carried out a computational fluid dynamics (CFD) numerical analysis and proposed a quasi-multidimensional transient model for an air-to-air counter-flow shell-and-tube MEE. Comparing the dew point temperature of MEE output between this research and experimental studies showed the accuracy of this method. They examined the effect of membrane thickness, flow rate, tube length, and temperature on MEE efficiency. Despite the change in flow rate, the vapor transfer rate was almost constant when the membrane thickness was greater than 150  $\mu\text{m}$ .

Ghaedamini et al. [16] in an experimental study, investigated the effects of flow rate, flow configuration, operating pressure, etc. on the efficiency of a counter-flow plate MEE whose channels are partially blocked by eight obstacles, with isothermal boundary conditions. By keeping the operating temperature of MEE and the dry channel flow rate constant, they concluded that using a partially blocked obstacle in wet channel enhances the WRR by 10 and 20%. It was also reported that it is necessary to put at least two obstacles in the channel to get better efficiency. Afshari and Houreh [17] used computational fluid dynamics (CFD) to analyze nickel metal foam as a humidifier flow distributor. They used three configurations in their study: Application of metal foam on the wet channel, the dry channel, and both channels. They showed that MEE combined with metal foam works better than conventional humidifiers due to the enhance in the residence time of gases in flow

channels. Further, the use of metal foam on dry and wet channels had higher efficiency at low flow rates, and use of metal foam on the wet channel had better efficiency at high flow rates. Houreh et al. [18] compared two three-dimensional MEEs, one of which had obstacles embedded in the channels. The results demonstrated that the average velocity in the channels with rectangular obstacles is 0.056 and 0.07 m/s, respectively, more than that in the channels with circular and triangular obstacles. Besides, the flow in the channel with a rectangular obstacle is 0.181 m/s more than that in the channel without obstacles, indicating the improvement of water transfer through the membrane in the channel with rectangular obstacles compared to the other cases.

Bhatia et al. [19] used the  $\varepsilon$ -NTU technique and considered mass transfer and heat transfer to analyze the temperature and concentration variations along an MEE numerically. They showed that ignoring mass transfer can lead to wrong results. Their results demonstrated that enhancing the molar rate of the dry channel improves the MEE efficiency. It also indicated that the dry channel exhaust RH is augmented linearly with the RH of the wet air entry. A 66% increase in the entry pressure of the dry channel also improved the efficiency of the humidifier by 50%. Yu et al. [20] employed the  $\varepsilon$ -NTU technique to evaluate the effect of different parameters on the efficiency of a counter-flow plate MEE. Their results revealed that dew point at the dry channel exhaust increased with the channel surface. However, in certain cases, numerous channels with a small area can improve this parameter. Chen et al. [21] performed experimental and numerical analysis using the thermodynamic method to assess the efficiency of a shell-and-tube MEE and a transient model of a plate MEE. The results showed that the water pressure in the wet channel does not affect the steam transfer from the membrane and therefore, it can be ignored in the modelling of MEE. However, water transfer rate (WTR) is highly dependent on airflow velocity and temperature in such a way that WTR is enhanced with them.

Afshari and Houreh [22] assessed the effect of dimensional parameters affecting PEMFC efficiency, like hydraulic channel diameter, membrane surface, and membrane thickness, on dry channel exhaust dew point, WTR, WRR, etc., using the thermodynamic method. Their results revealed that an enhancement in the thickness of the membrane reduces the dry channel exhaust dew point, leading to a decrease in the overall efficiency of MEE. The increase in the mass flow rate on the dry and wet channels resulted in increasing in temperature of the wet channel exhaust and a decrease in the temperature of the dry channel exhaust. Enhancing the surface area of the membrane from 0 to 5 cm<sup>2</sup>

augmented the dry channel exhaust dew point quickly. As the surface area of the membrane became > 5 cm<sup>2</sup>, the dew point of the exhaust of the dry channel was enhanced slowly.

In the present study, thermodynamic modelling of a plate air-to-air MEE with square channels is performed using a PEMFC by applying EES software. The governing equations, including a system of three nonlinear coupled equations, along with several dependent equations, are solved until the appropriate convergence is reached. This study aims to increase the accuracy of solving equations compared to previous studies. The innovations of the present study are as follows:

- To examine effective parameters, for the first time, the present study presents the exergy efficiency, including thermodynamic exergy, chemical exergy, and mechanical exergy, for MEE used for PEMFC applications.
- The pressure drop along the channels is considered as one of the equations according to Darcy's law.
- The specific heat capacity  $C_p$  is assumed to be a function of temperature in the calculations.
- The conduction heat transfer coefficient in the membrane is considered in the code, unlike previous studies.
- The sensitivity analysis is carried out based on four efficiency evaluation criteria, including WRR, effectiveness, entropy generation, and exergy efficiency. When four criteria show positive impacts by enhancing each parameter, A rating is assigned to that parameter, representing the optimal efficiency. When three, two and one criteria experience positive impacts, the ranks of B, C, and D are assigned to the considered parameter.
- A comprehensive parametric study, including investigating the effects of wet channel entry temperature for three relative humidities in the wet channel entry, dry channel entry pressure for three dry channel entry temperatures, the entry pressure of dry channel at three temperatures, the entry pressure of the wet channel at three temperatures, and RH at the entry of the dry channel at three temperatures are performed.

## 2 Modelling

Figure 1 shows the schematic of the plate MEE. According to Figure 1, dry air enters the dry channel (control volume 1) and the mixture of hot and humid water vapor and air enters the wet channel (control volume 2). Moisture and heat are transferred from the wet channel (steam) to the dry channel through diffu-

sion due to the difference in water concentration and temperature on both channels of the membrane.

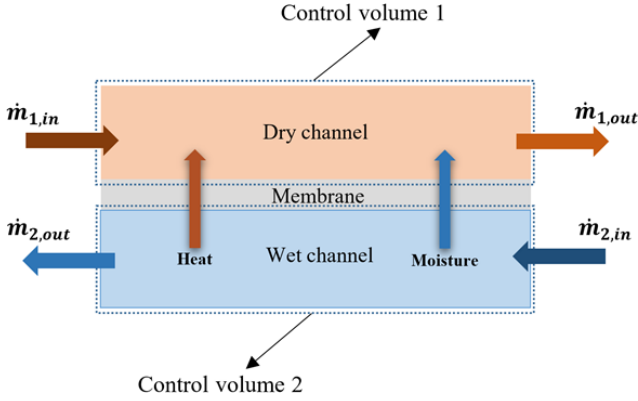


Fig. 1. Schematic of a counter flow plate MEE.

## 2.1 Assumptions

- i. The flow in MEE channels is laminar and incompressible since Reynolds number ( $\Re < 2000$ ).
- ii. Entry gases and vapors are ideal gases.
- iii. The outer walls of MEE are completely insulated and heat transfer between gases is done only through the membrane.
- iv. The effect of gravity is ignored.
- v. The fluid flow in the MEE is in a steady state.
- vi. The membrane only passes heat and water vapor and is impermeable to other gases.

## 2.2 Flow governing equations

The first law of thermodynamics for the control volumes 1 and 2 is expressed in Equations (1) and (2), respectively:

$$\begin{aligned} \dot{m}_{1,\text{air},\text{out}} h_{1,\text{air},\text{out}} + \dot{m}_{1,\text{v},\text{out}} h_{1,\text{v},\text{out}} \\ = \dot{q} + \dot{m}_{1,\text{air},\text{in}} h_{1,\text{air},\text{in}} \\ + \dot{m}_{1,\text{v},\text{in}} h_{1,\text{v},\text{in}} + \text{WTR} h_{\text{mem}}, \end{aligned} \quad (1)$$

$$\begin{aligned} \dot{m}_{2,\text{air},\text{out}} h_{2,\text{air},\text{out}} + \dot{m}_{2,\text{v},\text{out}} h_{2,\text{v},\text{out}} \\ = -\dot{q} + \dot{m}_{2,\text{air},\text{in}} h_{2,\text{air},\text{in}} \\ + \dot{m}_{2,\text{v},\text{in}} h_{2,\text{v},\text{in}} + \text{WTR} h_{\text{mem}}. \end{aligned} \quad (2)$$

Here,  $\dot{m}_{1,\text{air},\text{out}}$ ,  $\dot{m}_{1,\text{v},\text{out}}$ ,  $\dot{m}_{1,\text{air},\text{in}}$  and  $\dot{m}_{1,\text{v},\text{in}}$  indicate the exhaust and entry mass flow rates of air and water vapor to the control volume 1, respectively.  $\dot{m}_{2,\text{air},\text{out}}$ ,  $\dot{m}_{2,\text{v},\text{out}}$ ,  $\dot{m}_{2,\text{air},\text{in}}$  and  $\dot{m}_{2,\text{v},\text{in}}$  are the exhaust and entry mass flow rates of air and water vapor to the control volume 2, respectively.  $\dot{q}$  is the heat transfer rate and WTR is the mass transfer rate of water vapor through the membrane from the control volume 2 to 1.  $h_1$  and  $h_2$  are enthalpy in control volumes 1 and 2, respectively.

The subscripts  $v$ ,  $\text{air}$ , and  $\text{MEE}$  refer to vapor, air, and membrane, respectively. Equation (3) is obtained by writing the mass conservation equation [22, 23]:

$$\dot{m}_{2,\text{v},\text{in}} - \dot{m}_{2,\text{v},\text{out}} = \text{WTR} = \dot{m}_{1,\text{v},\text{out}} - \dot{m}_{1,\text{v},\text{in}}. \quad (3)$$

$h_{\text{mem}}$  expresses the enthalpy of the membrane and is obtained as follows:

$$h_{\text{mem}} = C_{p,v} T_{\text{mem}}, \quad (4)$$

where  $C_{p,v}$  is the specific heat of vapor and  $T_{\text{mem}}$  is the membrane temperature, which is calculated based on the average entry and exhaust temperatures of the two channels:

$$T_{\text{mem}} = \frac{T_{1,\text{out}} + T_{1,\text{in}} + T_{2,\text{out}} + T_{2,\text{in}}}{4}, \quad (5)$$

where  $T_{1,\text{in}}$  and  $T_{2,\text{in}}$  are the temperature of the fluid entering the dry and wet channels, respectively, and  $T_{1,\text{out}}$  and  $T_{2,\text{out}}$  are the temperature of the fluid exiting the dry and wet channels, respectively. The moisture transfer rate of the membrane is obtained as [24]:

$$\text{WTR} = D_w A \frac{C_2 - C_1}{0.5 t_m} M_v. \quad (6)$$

Here,  $M_v$  is the molar mass of water,  $A$  is the area of the membrane, and  $t_m$  is the thickness of the membrane.  $D_w$  is the moisture diffusion coefficient that is calculated using empirical Equation (7):

$$D_w = D_\lambda \exp \left[ 2416 \left( \frac{1}{303} - \frac{1}{T_{\text{mem}}} \right) \right], \quad (7)$$

where  $D_\lambda$  is estimated as follows [23]:

$$D_\lambda = \begin{cases} 3.1 \times 10^{-7} \lambda_m (e^{0.28\lambda} - 1) e^{-\frac{2346}{T_{\text{mem}}}} & 0 \leq \lambda_m \leq 3 \\ 4.17 \times 10^{-8} \lambda_m (1 + 161 e^{-\lambda}) e^{-\frac{2346}{T_{\text{mem}}}} & \lambda_m > 3 \end{cases} \quad (8)$$

Here,  $\lambda_m$  is the water capacity of the membrane that is calculated according to Equation (9):

$$\lambda_m = 0.043 + 17.81 a_m - 39.85 a_m^2 + 36 a_m^3. \quad (9)$$

In this equation,  $a_m$  is the RH of the membrane that is determined as follows:

$$a_m = \frac{\phi_1 + \phi_2}{2}. \quad (10)$$

Here,  $\phi_1$  and  $\phi_2$  are the RH of the control volumes 1 and 2, respectively:

$$\phi_1 = \phi_{1,\text{out}} = \frac{P_{1,\text{out}} \omega_{1,\text{out}}}{P_{1,\text{sat}} (\omega_{1,\text{out}} + \beta)}, \quad (11)$$

$$\phi_2 = \phi_{2,\text{out}} = \frac{P_{2,\text{out}} \omega_{2,\text{out}}}{P_{2,\text{sat}} (\omega_{2,\text{out}} + \beta)}, \quad (12)$$

where

$$\beta = \frac{M_v}{M_{\text{air}}}. \quad (13)$$

Here,  $M_v$  is the molar mass of vapor and  $M_{\text{air}}$  is the molar mass of air.

$C_1$  and  $C_2$  are the water concentrations on both channels of the membrane that are obtained as follows:

$$C_1 = \frac{\rho_{m,\text{dry}}}{W_{m,\text{dry}}} \lambda_1, \quad (14)$$

$$C_2 = \frac{\rho_{m,\text{dry}}}{W_{m,\text{dry}}} \lambda_2, \quad (15)$$

where  $\rho_{m,\text{dry}}$  is the dry density of the membrane, and  $W_{m,\text{dry}}$  is the dry weight of the membrane.  $\lambda_1$  and  $\lambda_2$  are the water capacity in the control volumes 1 and 2:

$$\lambda_1 = 0.043 + 17.81 \phi_{1,\text{out}} - 39.85 \phi_{1,\text{out}}^2 + 36 \phi_{1,\text{out}}^3, \quad (16)$$

$$\lambda_2 = 0.043 + 17.81 \phi_{2,\text{out}} - 39.85 \phi_{2,\text{out}}^2 + 36 \phi_{2,\text{out}}^3. \quad (17)$$

The heat transfer rate between the control volumes 1 and 2 is obtained using Equation (18):

$$\dot{q} = UA\Delta T_{\text{LM}}, \quad (18)$$

where  $\Delta T_{\text{LM}}$  is the logarithmic mean temperature difference that is calculated as follows for the counter-flow MEE:

$$\begin{aligned} T_{\text{LM}} &= \frac{\Delta T_{\text{in}} - \Delta T_{\text{out}}}{\ln\left(\frac{\Delta T_{\text{in}}}{\Delta T_{\text{out}}}\right)} \\ &= \frac{(T_{2,\text{in}} - T_{1,\text{out}}) - (T_{2,\text{out}} - T_{1,\text{in}})}{\ln\left(\frac{T_{2,\text{in}} - T_{1,\text{out}}}{T_{2,\text{out}} - T_{1,\text{in}}}\right)}. \end{aligned} \quad (19)$$

Here,  $A$  is the cross-sectional area of the membrane.  $U$  is the overall heat transfer coefficient that is obtained using the Nusselt number (Nu):

$$\frac{1}{U} = \frac{D_h}{\text{Nu} k_{\text{air}}} + \frac{D_h}{\text{Nu} k_v} + \frac{t_m}{k_{\text{mem}}} \quad (20)$$

Here,  $k_{\text{air}}$ ,  $k_v$  and  $k_{\text{mem}}$  are the thermal conductivity of the dry channel, wet channel, and membrane respectively, and  $D_h$  is the hydraulic diameter of the channel. The total heat transfer rate and  $D_h$  for a square cross-section are determined as follows:

$$\dot{Q}_{\text{rate}} = \frac{Q \times 1000}{A_{\text{mem}}}, \quad (21)$$

$$D_h = \frac{4a^2}{4a} = a, \quad (22)$$

where  $a$  is the channel length of the square channel. The specific heat constant at constant pressure for air and water vapor is obtained as:

$$\begin{aligned} C_{p,\text{air}} &= \left[ 1.05 - 0.365 \times \frac{T}{1000} + 0.85 \times \left(\frac{T}{1000}\right)^2 \right. \\ &\quad \left. - 0.39 \times \left(\frac{T}{1000}\right)^3 \right] \times 1000, \end{aligned} \quad (23)$$

$$\begin{aligned} C_{p,v} &= \left[ 1.79 - 0.107 \times \frac{T}{1000} + 0.586 \times \left(\frac{T}{1000}\right)^2 \right. \\ &\quad \left. - 0.2 \times \left(\frac{T}{1000}\right)^3 \right] \times 1000, \end{aligned} \quad (24)$$

where  $T$  is the temperature (K).

The humidity ratio at the exhaust of dry and wet channels is obtained using the following equations:

$$\omega_{1,\text{out}} = \frac{\dot{m}_{1,v,\text{out}}}{\dot{m}_{1,\text{air},\text{out}}}, \quad (25)$$

$$\omega_{2,\text{out}} = \frac{\dot{m}_{2,v,\text{out}}}{\dot{m}_{2,\text{air},\text{out}}}. \quad (26)$$

The saturation pressure at any point of the dry and wet channel is obtained as follows [18]:

$$P_{\text{sat}} = 0.61078 \exp\left(\frac{17.27T}{T + 237.3}\right) \quad (27)$$

where  $P_{\text{sat}}$  is in kPa and  $T$  is in K.

The pressure drop (Pa) in the flow path is calculated as:

$$\Delta P = \rho f \frac{L}{D_h} \frac{V^2}{2} \quad (28)$$

Here,  $f$  is the friction coefficient,  $L$  is the length of the flow path (channel length), and  $V$  is the fluid flow velocity.

## 2.3 Numerical method

According to the previous section, a system of three nonlinear coupled equations along with several dependent equations should be solved. By solving Equations (1), (2), and (6), three unknowns are obtained: Wet channel exhaust temperature ( $T_{2,\text{out}}$ ), dry channel exhaust temperature ( $T_{1,\text{out}}$ ), and moisture transfer rate from the membrane (WTR). To solve these system of nonlinear coupled equations, EES software is used. The iteration method is employed to reach the appropriate convergence (residual of  $10^{-4}$ ). Table 1 presents the material properties and operating conditions of MEE.

**Table 1. Properties of MEE materials and operating conditions.**

Parameter	Unit	Value
Entry mass flow to the dry and wet channel ( $\dot{m}$ )	kg/s	$5 \times 10^{-6}$
Dry channel entry temperature ( $T_{\text{dry,in}}$ )	K	303
Wet channel entry temperature ( $T_{\text{wet,in}}$ )	K	353
Dry channel entry relative humidity ( $\text{RH}_{\text{dry,in}}$ )	%	0
Wet channel entry relative humidity ( $\text{RH}_{\text{wet,in}}$ )	%	100
Operating pressure ( $P$ )	kPa	101.325
Equivalent weight of the membrane in the dry state ( $W_{m,\text{dry}}$ )	kg mol <sup>-1</sup>	1
Membrane density in the dry state ( $\rho_{m,\text{dry}}$ )	kg m <sup>-3</sup>	100
Membrane area ( $A_{\text{mem}}$ )	m <sup>2</sup>	$410 \times 10^{-4}$
Membrane porosity ( $\mathcal{E}$ )	-	0.5
Membrane permeability ( $K$ )	m <sup>2</sup>	$1 \times 10^{-10}$
Thermal conductivity of dry air ( $k_{\text{air}}$ )	Wm <sup>-1</sup> K <sup>-1</sup>	0.02816
Thermal conductivity of wet air ( $k_v$ )	Wm <sup>-1</sup> K <sup>-1</sup>	0.02831

### 2.3.1 The main criteria for evaluating the MEE efficiency

#### Dry channel exhaust temperature ( $T_{1,\text{out}}$ )

**WTR** It is defined in Equation (6).

**WRR** The ratio of the rate of water transferred from the wet channel to the dry channel to the flow rate of the entry water on the wet channel [25]. Higher WRR leads to better MEE efficiency. In some studies, WRR is also called MEE efficiency [19]. WRR is defined as follows:

$$\text{WRR} = \frac{\text{WTR}}{\dot{m}_{2,v,\text{in}}} \quad (29)$$

**Exergy efficiency ( $\eta_{\text{ex}}$ )** : The maximum work that a system can do during the process takes place from the initial state to the dead state, which is called exergy. In all thermodynamic processes, the aim is to reduce entropy generation and exergy to obtain higher efficiency. The first and second laws of thermodynamics are widely used in engineering systems, and exergy

analysis is a combination of these two laws. In the efficiency analysis of an MEE, entropy, and exergy analysis can also be used to evaluate heat and mass transfer losses [26]. Exergy destruction consists of three parts: (i) thermodynamic exergy, (ii) chemical exergy, and (iii) mechanical exergy.

The maximum possible work to change the temperature and pressure compared to the ambient temperature and pressure without changing the concentration is called thermodynamic exergy. The thermodynamic exergy of air is as follows [26]:

$$\text{ex}_{\text{th,air}}(T) = (C_{p,\text{air}} + \omega C_{p,v})T_0 \left( \frac{T}{T_0} - 1 - \ln \frac{T}{T_0} \right) \quad (30)$$

The maximum possible work to reach the concentration of the system to the concentration of the environment is called chemical concentration and is defined as follows [26]:

$$\text{ex}_{\text{ch}}(\omega) = RT_0 \left[ (1 + 1.608\omega) \ln \frac{1 + 1.608\omega_0}{1 + 1.608\omega} + 1.608\omega \ln \frac{\omega}{\omega_0} \right]. \quad (31)$$

Flow resistance is the cause of mechanical exergy. Mechanical exergy is defined as follows:

$$\text{ex}_{\text{me,air}}(P) = (1 + 1.608\omega)RT_0 \ln \frac{\omega}{\omega_0}. \quad (32)$$

The exergy equation for the mixture of air and water vapor is written as the sum of thermodynamic, chemical, and mechanical exergies [26]:

$$\begin{aligned} \text{Ex} = & \dot{m}(C_{p,\text{air}} + \omega C_{p,v})T_0 \left( \frac{T}{T_0} - 1 - \ln \frac{T}{T_0} \right) \\ & + (1 + 1.608\omega)R_a T_0 \ln \frac{P}{P_0} \\ & + R_a T_0 (1 + 1.608\omega) \ln \frac{1 + 1.608\omega_0}{1 + 1.608\omega} \\ & + 1.608\omega \ln \frac{1.608\omega}{1.608\omega_0}, \end{aligned} \quad (33)$$

where  $\omega$  is the humidity ratio and  $R_a$  is the air gas constant. Exergy efficiency is calculated as follows:

$$\eta_{\text{Ex}} = \frac{\text{Ex}_{\text{product}}}{\text{Ex}_{\text{fuel}}}, \quad (34)$$

where

$$\text{Ex}_{\text{product}} = \text{Ex}_{1,\text{out}} - \text{Ex}_{1,\text{in}}, \quad (35)$$

$$\text{Ex}_{\text{fuel}} = \text{Ex}_{2,\text{in}} - \text{Ex}_{2,\text{out}}. \quad (36)$$

**Entropy generation ( $S_{\text{generate}}$ )** Entropy generation indicates irreversibility during heat and mass transfer. In the thermodynamic design of heat exchangers, minimizing entropy generation is a suitable feature for design optimization. Entropy generation originates from three factors: (i) heat transfer between the dry and wet channels, (ii) moisture transfer between the dry and wet channels, and (iii) flow resistance. The entropy generation of the whole system is calculated as follows [26]:

$$S_{\text{generate}} = \left[ (\dot{m}_{1,\text{in}} + \text{WTR}) S_{1,\text{out}} \right] + \left[ (\dot{m}_{2,\text{in}} - \text{WTR}) S_{2,\text{out}} \right] - \left[ (\dot{m}_{1,\text{in}} S_{1,\text{in}}) + (\dot{m}_{2,\text{in}} S_{2,\text{in}}) \right]. \quad (37)$$

Here,  $S_{1,\text{in}}$  and  $S_{1,\text{out}}$  are the entropy at the entry and exhaust of the dry channel.  $S_{2,\text{in}}$  and  $S_{2,\text{out}}$  are the entropy at the entry and exhaust of the wet channel.

**Effectiveness** This is a key performance metric for evaluating the humidification efficiency of MEE's in fuel cell systems. It is defined as the ratio of the actual temperature rise of the dry inlet air to the maximum possible temperature rise. It is obvious that the performance of MEE increases with increasing effectiveness. Effectiveness is defined as follows [27, 28]:

$$\varepsilon = \frac{T_{1,\text{in}} - T_{1,\text{out}}}{T_{1,\text{in}} - T_{2,\text{in}}}. \quad (38)$$

## 2.4 Validation of the numerical model

The same conditions and properties are adopted for the numerical model according to the experimental study conducted by Baharlou Hourah et al. [14]. There is a good agreement between the numerical and experimental results with a deviation of less than 3.5% for WRR and less than 1% for temperature (see Figure 2).

## 3 Results

### 3.1 Effect of wet channel entry temperature for different wet channel entry relative humidities

Since the temperature of the wet air exiting from the cathode side of the PEMFC is between 343 and 353 K and its humidity is between 80 and 100% and it is placed as the input of the wet channel in the MEE, the temperature and RH are examined at these ranges of parameters.

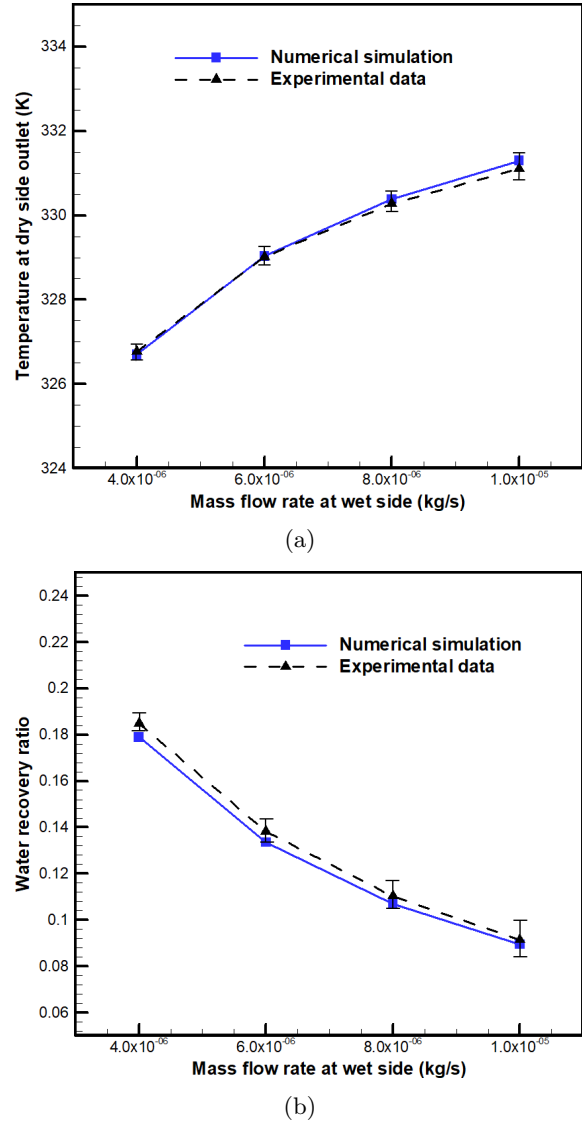


**Fig. 2. Comparison between numerical simulation results and experimental data [14]: (a) exhaust temperature of dry channel and (b) WRR.**

Considering Figure 3a, increasing temperature of the wet channel exhaust leads to an enhancement in temperature at the dry channel exhaust with an almost linear relevance. An enhancement in the RH of the entry of the wet channel also increases the dry channel exhaust temperature. Figure 3b demonstrates that the WTR is enhanced significantly with the entry temperature of the wet channel at a constant RH. According to Equation (6), because the denominator of the fraction increases and RH is constant, the numerator increases, enhancing the flow rate of the entry water on wet channel; hence, WTR should also be increased. Moreover, at a constant temperature, an increase in RH on wet channel leads to a small enhancement in moisture transfer in the membrane. According to Fig-

ure 3c, increasing both temperature and RH parameters increases the effectiveness. It is concluded from Figure 3d that as the temperature at wet channel entry is increased from 343 to 353 K, the WRR is reduced by 2%. When the entry temperature of the wet channel is augmented, according to Equation (27),  $P_{\text{sat}}$  is enhanced. Since RH is constant, when the denominator of the fraction increases, the numerator of the fraction ( $P_v$ ) increases. Therefore, at a certain RH, the flow rate of the entry water of the wet channel increases with the entry temperature of the wet channel. Therefore, it is seen from Equation (29) that the denominator of the fraction increases, leading to a decrease in WRR.

On the other hand, according to Figure 3b, the increase in the WTR due to the enhanced temperature of the wet channel entry can augment the WRR. Therefore, it can be stated that the effect of the entry water flow on wet channel overcomes the effect of WTR, re-

sulting in a decrease in WRR. Besides, according to Figure 3d, at a constant temperature, enhancing the RH at the entry of the wet channel leads to an 11.1% decrease in WRR. For example, at a temperature of 343 K, WRR is 70%, 67.5%, and 63% for relative humidities of 80%, 90%, and 100%, respectively. The constant temperature means that the saturation pressure is constant because the saturation pressure is only dependent on the temperature. Thus, there is a direct relation between RH and  $P_v$ : An increase in RH results in an increase in  $P_v$ . Thus, the entry water flow toward the wet channel ( $\dot{m}_{2,v,\text{in}}$ ) increases, leading to a decrease in WRR according to Equation (29). Although Figure 3b demonstrates that the increase in RH at the wet channel entry enhances the WTR, the WRR decreases due to the dominance of the water flow rate at the wet channel entry more than effect of the WTR.

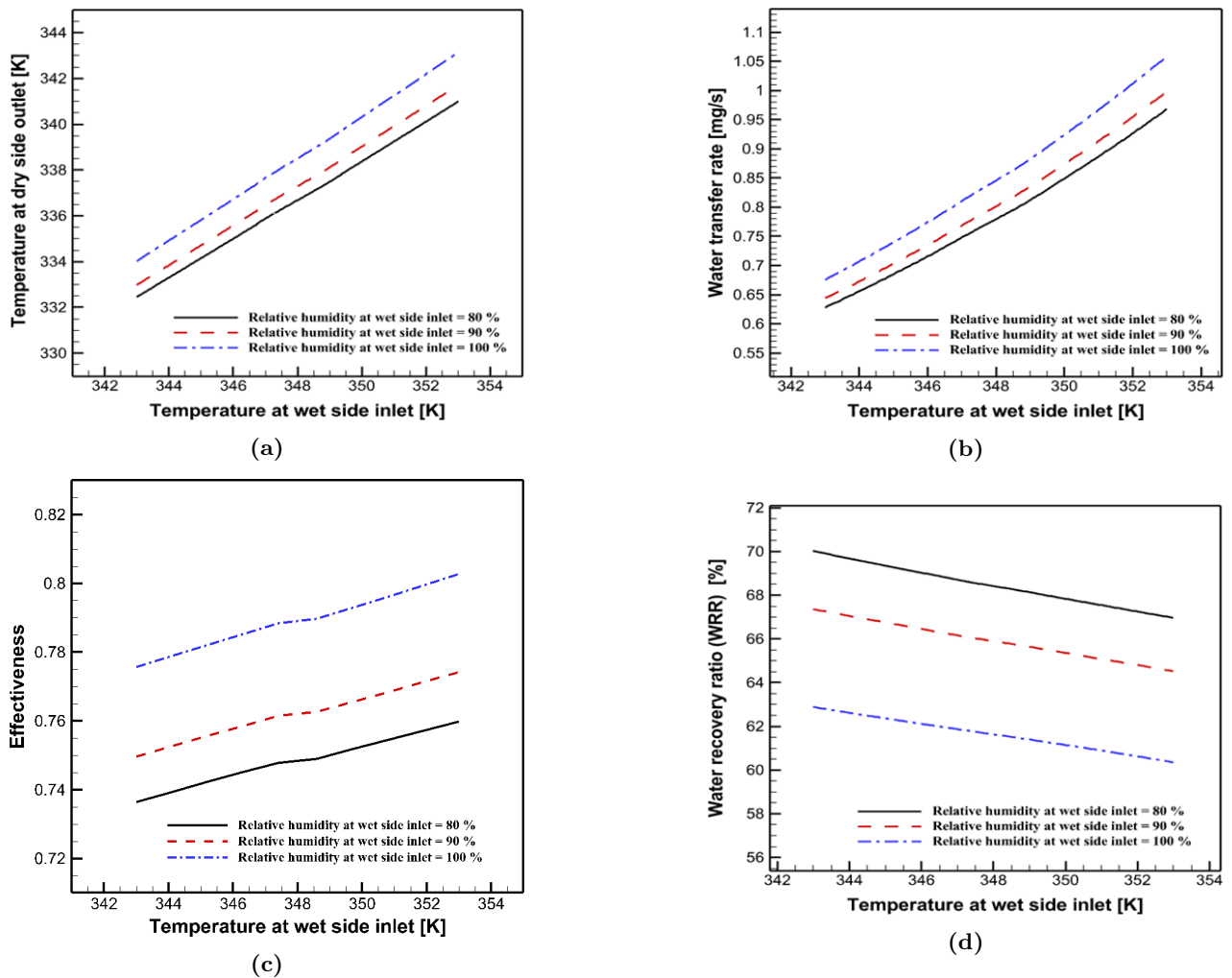


Fig. 3. Effect of temperature and relative humidity of the entry of the wet channel on (a) exhaust temperature of the dry channel, (b) water transfer rate from the membrane, (c) Effectiveness and (d) WRR.

According to Figure 4a, the exergy efficiency is improved by 1.25% and then decreased by 3.9% with the entry temperature of the wet channel. The maximum exergy efficiency corresponds to the temperature of 348 K. Also, an enhancement in the RH from 80 to 100% reduces the exergy efficiency by 11.8%. Fig-

ure 4b reveals that the rate of entropy generation increases with the temperature and wet channel entry RH, indicating the increase in the irreversibility of heat transfer. According to Figure 4b, as the entry RH becomes closer to 100%, the entropy enhancement slope becomes greater.

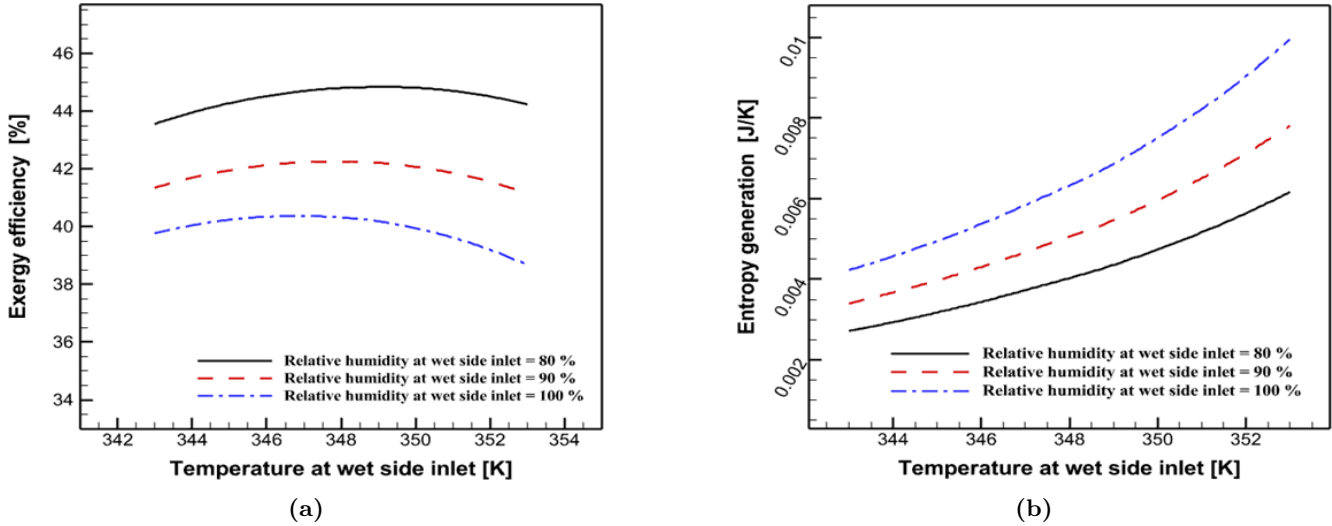


Fig. 4. Effect of temperature and relative humidity of the entry of the wet channel on (a) exergy efficiency and (b) entropy generation.

### 3.2 Effect of the relative humidity of the dry channel entry at different temperatures of the dry channel entry

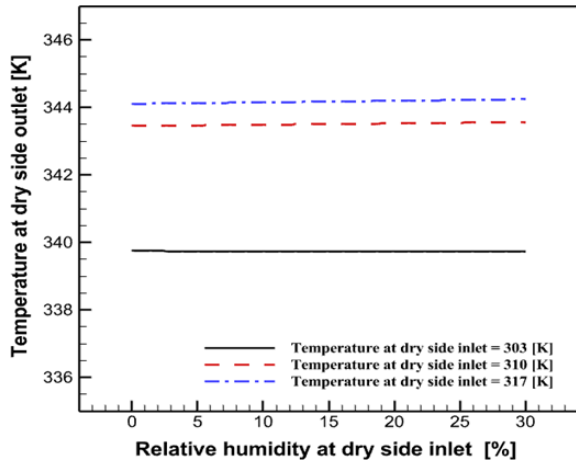
Ambient air is usually used in most regions to enter the MEE's dry channel. This air is usually not dry and contains some moisture. In this section, the RH of the dry channel entry is considered to be between 0 and 30%. According to Figure 5a, an enhancement in the RH of the entry of the dry channel does not affect the exhaust temperature of the dry channel. By increasing the temperature of the entry gas from 303 to 317 K, the exhaust temperature of the dry channel is enhanced from 339.5 K to 344 K. As can be seen from Figure 5b, increasing the RH of the inlet of the dry side will not affect the effectiveness. The comparison of the effect of increasing the dry side inlet temperature on the effectiveness in this figure shows that the temperatures of 310, 317 and 303 K are the most effective, respectively. According to Figure 5c, increasing the RH of the dry channel entry from 0 to 30% leads to a reduction in the WRR from 2.5% for the temperature of the dry channel entry of 303 K to 4.5% for the dry channel entry temperature of 317 K. According to Equation (29), there is a direct relationship between WTR and WRR due

to constant conditions at the wet channel entry, and as a result, their variations are consistent. Further, enhancing the temperature of the entry gas on the dry channel increases the WRR by 30.5%.

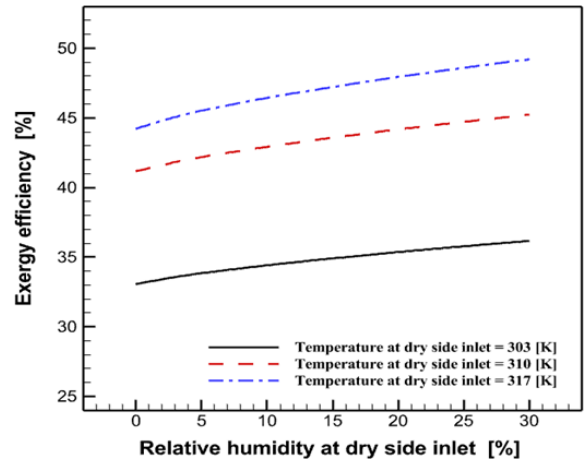
According to Figure 6a, the increase in RH and the temperature of the entry gas of the dry channel improves the exergy efficiency. It is observed that the effect of increasing temperature is greater than that of increasing RH. By increasing the RH from 0 to 30%, the exergy efficiency is improved by 3% at the temperature of the dry channel entry of 303 K. For a certain RH, for example, 0%, the exergy efficiency is augmented from 33% to 44% with an increment in the temperature at the dry channel entry from 303 to 317 K. The enhancement in the RH of the dry channel entry, according to Figure 6b, results in a slight increase in the entropy generation of the whole system. Besides, increasing the entry temperature reduces the entropy generation.

### 3.3 Effect of dry channel entry pressure at different dry channel entry temperatures

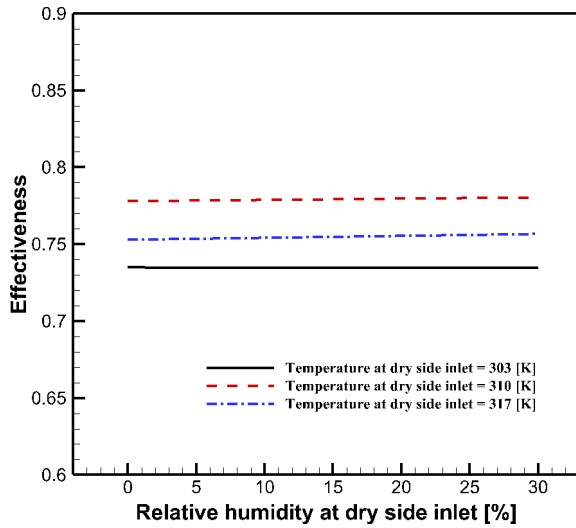
The entry pressure to the dry channel varies from 1 to 1.5 bar and its entry temperature changes from 306 to 318 K for the simulations illustrated in Figure 7a.



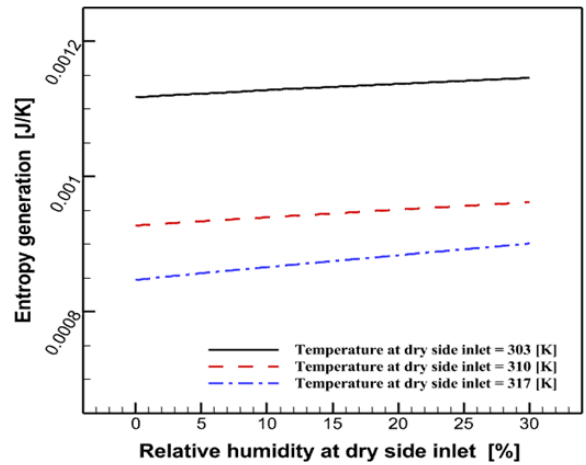
(a)



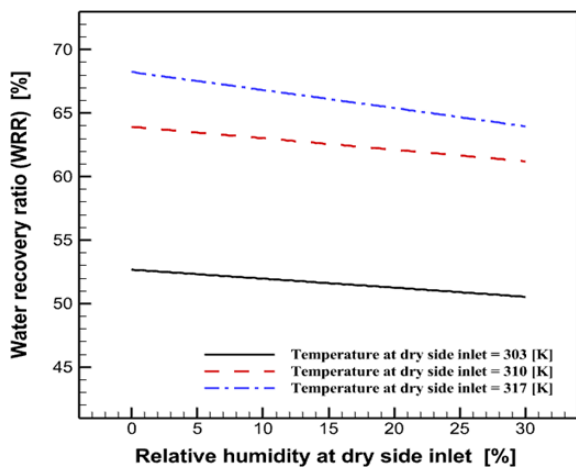
(a)



(b)



(b)



(c)

Fig. 5. Effects of relative humidity and dry channel entry temperature on (a) dry channel exhaust temperature, (b) Effectiveness and (c) WRR.

Fig. 6. Effects of relative humidity and dry channel entry temperature on (a) exergy efficiency and (b) entropy generation.

With the increase of pressure and temperature at the dry channel entry, the exhaust temperature of the dry channel increases. The influences of the increase in pressure are much greater than the increase in temperature. According to Figure 7b, increasing the inlet pressure of the dry side from 1 to 1.5 bar increases the effectiveness by approximately 14.5%, and the effectiveness also increases with the increase of the inlet temperature of the dry side. Figure 7c demonstrates that WRR declines by 22.8% by increasing the pressure at the dry channel entry. This is due to the effect of the pressure difference created between the dry and wet channels. Since the direction of moisture transfer is from wet channel to the dry channel, more pressure on the dry channel causes resistance to mass transfer. According to Equation (29), since the entry water flow to wet channel is constant, there is a direct relation between WTR and WRR. As seen in this figure, the WRR is enhanced with the increase in entry temper-

ature of the dry channel at a constant pressure. The results presented in this figure are consistent with the results of Bhatia et al. [19].

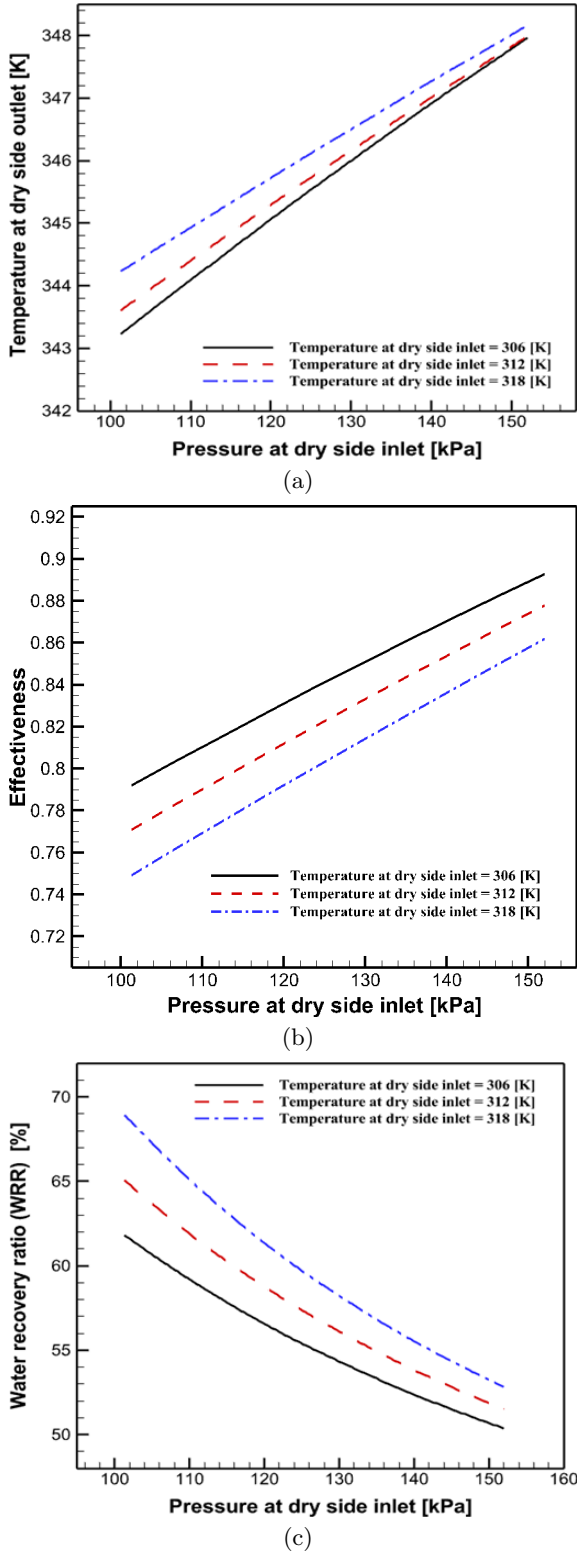


Fig. 7. Effects of pressure and temperature at the dry channel entry on (a) exhaust temperature of the dry channel, (b) Effectiveness and (c) WRR.

According to Figure 8a, the exergy efficiency is improved by more than 5% by increasing the dry channel entry pressure from 1 to 1.5 bar when the entry air temperature is 306 K. When the temperature at the dry channel entry is 318 K, the exergy efficiency is improved by less than 3%. Increasing the entry temperature from 306 to 318 K leads to an improvement in the exergy efficiency by 1 to 3% for different pressures. According to Figure 8b, enhancing the pressure at the channel entry results in an increase in entropy generation. An enhancement in the temperature leads to a decrease in the amount of entropy generated by the system.

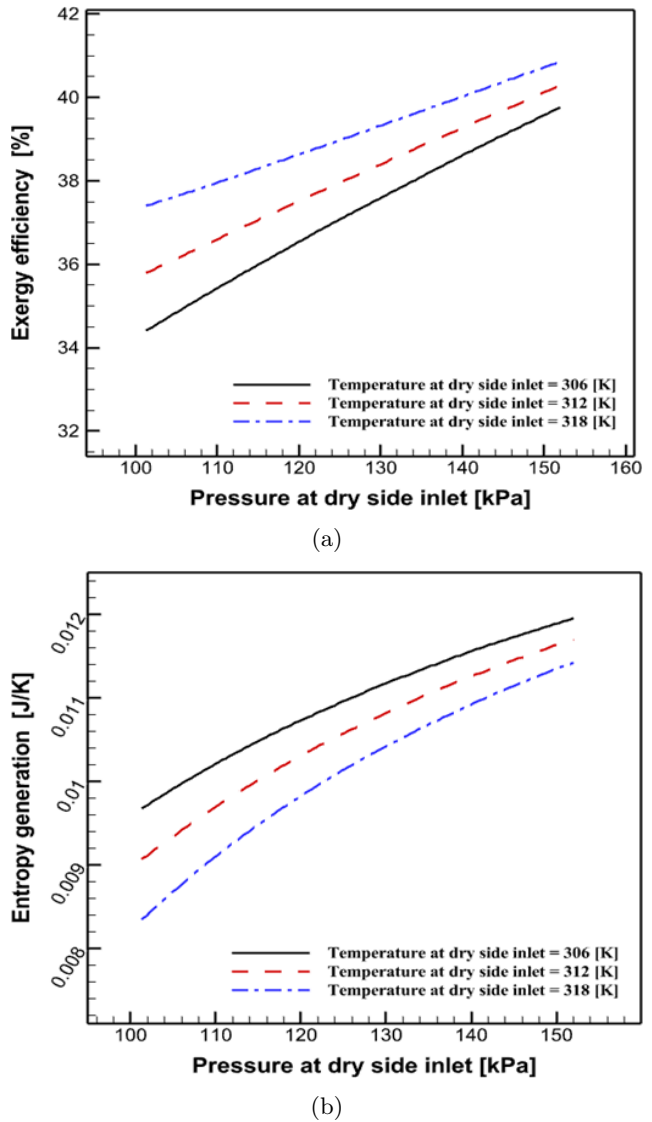


Fig. 8. Effects of pressure and temperature of the dry channel entry on (a) exergy efficiency and (b) entropy generation.

### 3.4 Effects of wet channel entry pressure

The effect of entry pressure of the wet channel changes from 1 to 2 bar on performance evaluation criteria at the dry inlet temperature of 303 K, which is shown in Figure 9. Considering Figure 9a, the dry channel exhaust temperature is reduced up to a certain pressure by increasing the entry pressure of the wet channel. Then, the temperature remains almost constant. Besides, the WTR is diminished slightly with the increase of pressure from 101.325 to 160 kPa at the wet channel entry. By enhancing the pressure from 160 to 203 kPa, the WTR decreases sharply. According to Figure 9b, increasing the inlet pressure of the wet side from 1 to 2 bar slightly reduces the effectiveness. Figure 9b also demonstrates that the WRR is increased by almost 35% with the increase of the wet channel entry pressure from 100 to 170 kPa. Then, by varying the pressure from 170 to 200 kPa, the WRR remains almost constant. According to Figure 9c, the exergy efficiency is improved by enhancing the entry pressure of the wet channel from 1 to 1.65 bar, but from this pressure onwards, exergy efficiency decreases drastically. As well, an increment in the pressure of the wet channel reduces the entropy generation at all values of wet channel entry pressure.

## 4 Comprehensive evaluation of studied parameters

To provide a comprehensive evaluation of the parameters investigated in this research, the effect of each parameter on the four evaluation criteria is presented in Table 2. If the increase of each parameter has a positive effect on four criteria, the A rating is assigned to the parameter. If it has a positive effect on three, two, or one criterion, the B, C, and D ratings, are assigned, respectively. The parameter with an A rating enhances WRR and effectiveness, improves exergy efficiency, and reduces entropy generation. Therefore, it is suggested that the parameters with the A rating should be used as much as possible in operating conditions, and the parameters with the D rating should be used as low as possible in operating conditions. Hence, an enhancement in the dry channel exhaust temperature results in the best efficiency in terms of four evaluation criteria. Although increasing the RH of the wet channel with a D rating leads to poor MEE efficiency, it cannot be limited to achieving the required water transfer rate. On the other hand, if a recirculation system is used, since the wet channel entry is the same as the exhaust of the cathode side of the PEMFC, changing its RH requires spending equipment and money. According to Table 2, a thinner membrane results in the best efficiency, but mechanical limitations like buckling,

tearing, and membrane life should be considered.

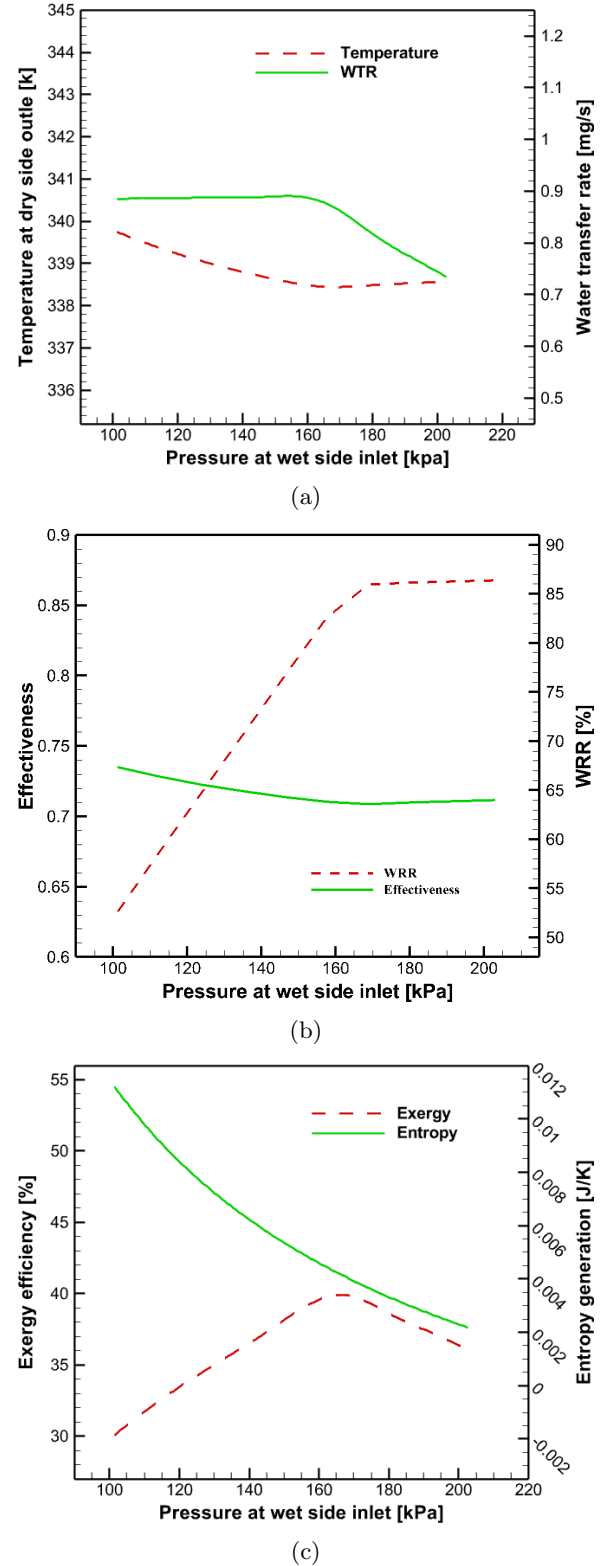


Fig. 9. Effects of pressure of the wet channel on (a) exhaust temperature of the dry channel & WTR, (b) Effectiveness & WRR and (c) exergy efficiency & entropy generation.

**Table 2.** Effect of increasing various parameters on the efficiency criteria of MEE (sign + indicates a positive effect and sign – shows a negative effect).

Efficiency criterion	Parameter	$S_{\text{generate}}$	$\eta_{\text{Ex}}$	WRR	Effectiveness	Rank
	$T_{2,\text{in}}$ (343 – 353 K)	–	$\pm$	–	+	C
	$T_{1,\text{in}}$ (303 – 317 K)	+	+	+	$\pm$	A
	$\phi_{2,\text{in}}$ (80 – 100%)	–	–	–	+	D
	$\phi_{1,\text{in}}$ (0 – 30%)	–	+	–	Constant	D
	$P_{2,\text{in}}$ (1 – 2 bar)	+	$\pm$	+	–	B
	$P_{1,\text{in}}$ (1 – 2 bar)	–	+	–	+	C

## 5 Conclusions

In this study, an air-to-air plate MEE for the PEMFC application was modelled by utilizing a thermodynamic method. The governing equations, including a system of three nonlinear coupled equations, along with several dependent equations, are solved until the appropriate convergence is reached. To validate the numerical results, an experimental setup has been used. The innovations of the present research are the comprehensive analysis of operating parameters and their mutual impact analysis using energy analysis (heat and moisture transfer), examination of exergy destruction and entropy generation, and sensitivity analysis of the parameters by employing these criteria. If the increase of each parameter has a positive effect on four criteria, the A rating is assigned to the parameter. If it has a positive effect on three, two or one criteria, the B, C and D ratings are assigned respectively. The parameter with rating A enhances WRR and effectiveness, improves exergy efficiency and reduces entropy generation. Therefore, it is suggested that the parameters with the A rating be used as much as possible in operating conditions and the parameters with the D rating be used as low as possible in operating conditions. Some of the principal results of the present study are as below:

- Enhancing the wet channel entry temperature from 343 to 353 K leads to a 2% decrease in WRR (negative effect on MEE efficiency), an increase in effectiveness (positive effect on MEE efficiency)

and an increment in entropy generation (negative effect on MEE efficiency). Increasing in wet channel entry temperature from 343 to 348 K results in a 1.25% improvement in exergy efficiency (positive effect on MEE efficiency). Its variation from 348 to 353 K leads to a 3.9% decrement in exergy efficiency (negative effect on MEE efficiency). Therefore, increasing the wet channel entry temperature gets a C rating in the sensitivity analysis.

- An increment in the RH of the wet channel at entry from 80% to 100% leads to an 11.1% decrease in WRR, an increase in effectiveness, an 11.8% reduction in exergy efficiency, and an enhancement in entropy generation. Therefore, the enhancement in the RH of the wet channel entry receives a D rating in the sensitivity analysis. Although enhancing the RH of the wet channel leads to a D rating and poor MEE efficiency, it cannot be limited to achieving the required water transfer rate. On the other hand, if a cyclic system is used, since the wet channel at entry is the same as the exhaust of the cathode side of the PEMFC, setting the RH of the entry of the wet channel at values lower than 80% is not economical.
- An enhancement in the RH of the dry channel entry from 0 to 30% results in a 2.5 to 4.5% decrease in WRR, a 3% reduction in exergy efficiency, and an increase in entropy generation. It does not change the effectiveness. Therefore, the RH enhancement at the dry channel entry gets a

D rating in the sensitivity analysis.

- Enhancing the dry channel entry temperature from 306 to 318 K leads to a 30.5% increment in WRR, at first increases and then decreases the effectiveness, an 11% improvement in exergy efficiency and a decrease in entropy generation. Therefore, an enhancement in the dry channel entry temperature gets an A rating in the sensitivity analysis.
- An augmentation in the dry channel entry pressure from 1 to 2 bar leads to a 22.8% decrease in WRR, an increase in effectiveness, an improvement in exergy efficiency between 3 to 5%, and an increase in entropy generation. Therefore, increasing the entry pressure at the dry channel receives a C rating in the sensitivity analysis.
- Enhancing the entry pressure of the wet channel from 1 to 1.7 bar increases the WRR by 10 to 30% and decreases the effectiveness. Enhancing the entry pressure at the wet channel from 1 to 1.2 bar and 1.2 to 1.55 bar improves the exergy efficiency by 9% and decreases the exergy efficiency by 18.5%, respectively, when the dry channel entry temperature is 317 K. Additionally, an increment in the entry pressure of the wet channel from 1 to 2 bar reduces the entropy generation. Therefore, increasing the entry pressure of the wet channel gets a B rating in the sensitivity analysis.

## Acknowledgments

This work was supported by Shahid Rajaei Teacher Training University under grant number 5973/98 (4 July 2024).

## References

- [1] Ghanbarian A, Kermani MJ, Scholta J. Generalization of a CFD Model to Predict the Net Power in PEM Fuel Cells. *Hydrogen, Fuel Cell & Energy Storage*. 2019;6(1):23–37. Available from: [https://hfe.irost.ir/article\\_793.html](https://hfe.irost.ir/article_793.html). 154
- [2] Barzegari M, Ghadimi M, Habibnia M, Momenifar M, Mohammadi K. Developed endplate geometry for uniform contact pressure distribution over PEMFC active area. *Hydrogen, Fuel Cell & Energy Storage*. 2020;7(1):1–12. Available from: [https://hfe.irost.ir/article\\_902.html](https://hfe.irost.ir/article_902.html). 154
- [3] Duan Z, Zhan C, Zhang X, Mustafa M, Zhao X, Alimohammadisagvand B, et al. Indirect evaporative cooling: Past, present and future potentials. *Renewable and sustainable energy reviews*. 2012;16(9):6823–6850. 154
- [4] Bhatt P, Agarwal N, Chakraborty UK. Parameter Optimization of PEMFC with Genetic Algorithm. *New Mathematics & Natural Computation*. 2016;12(3). 154
- [5] Tang J, Cai C, Xiao T, Huang S. Support vector regression model for direct methanol fuel cell. *International Journal of Modern Physics C*. 2012;23(07):1250055. 154
- [6] Nguyen XL, Vu HN, Yu S. Parametric understanding of vapor transport of hollow fiber membranes for design of a membrane humidifier. *Renewable Energy*. 2021;177:1293–1307. 154
- [7] Huizing R. Design and membrane selection for gas to gas humidifiers for fuel cell applications [MSC thesis]. University of Waterloo; 2007. 154
- [8] Ramya K, Sreenivas J, Dhathathreyan K. Study of a porous membrane humidification method in polymer electrolyte fuel cells. *International Journal of hydrogen energy*. 2011;36(22):14866–14872. 154
- [9] Alldoor AK, Ma Z, Cooper P. Experimental investigation and performance evaluation of a mixed-flow air to air membrane enthalpy exchanger with different configurations. *Applied Thermal Engineering*. 2020;166:114682. 154

- [10] Janajreh I, Suwwan D, Hashaikeh R. Assessment of direct contact membrane distillation under different configurations, velocities and membrane properties. *Applied Energy*. 2017;185:2058–2073. [154](#)
- [11] Shamsizadeh P, Afshari E, Mosharaf-Dehkordi M. Design of membrane humidifier using obstacles in the flow channels for ventilator. *Applied Thermal Engineering*. 2021;196:117265. [154](#)
- [12] Yang C, Cao L, Yang J. Mathematical modeling of a three-compartment electro-reactor process with ion-exchange membranes for recycling and resource recovery of desulfurization residuals. *Journal of Electroanalytical Chemistry*. 2016;762:7–19. [154](#)
- [13] Wolfenstetter F, Kreitmair M, Schoenfeld L, Klein H, Becker M, Rehfeldt S. Experimental study on water transport in membrane humidifiers for polymer electrolyte membrane fuel cells. *International Journal of Hydrogen Energy*. 2022;47(55):23381–23392. [154](#)
- [14] Houreh NB, Ghaedamini M, Shokouhmand H, Afshari E, Ahmaditaba A. Experimental study on performance of membrane humidifiers with different configurations and operating conditions for PEM fuel cells. *International Journal of Hydrogen Energy*. 2020;45(7):4841–4859. [154](#), [159](#)
- [15] Park S, Jung D. Effect of operating parameters on dynamic response of water-to-gas membrane humidifier for proton exchange membrane fuel cell vehicle. *International journal of hydrogen energy*. 2013;38(17):7114–7125. [154](#)
- [16] Ghaedamini M, Houreh NB, Afshari E, Shokouhmand H, Ahmaditaba A. Experimental parametric study on performance of a membrane heat and moisture exchanger with partially blocked channels at isothermal condition. *Applied Thermal Engineering*. 2020;175:115400. [154](#)
- [17] Afshari E, Houreh NB. Performance analysis of a membrane humidifier containing porous metal foam as flow distributor in a PEM fuel cell system. *Energy conversion and management*. 2014;88:612–621. [154](#)
- [18] Houreh NB, Shokouhmand H, Afshari E. Effect of inserting obstacles in flow field on a membrane humidifier performance for PEMFC application: A CFD model. *International Journal of Hydrogen Energy*. 2019;44(57):30420–30439. [155](#), [157](#)
- [19] Bhatia D, Sabharwal M, Duell C. Analytical model of a membrane humidifier for polymer electrolyte membrane fuel cell systems. *International Journal of Heat and Mass Transfer*. 2013;58(1-2):702–717. [155](#), [158](#), [163](#)
- [20] Yu S, Im S, Kim S, Hwang J, Lee Y, Kang S, et al. A parametric study of the performance of a planar membrane humidifier with a heat and mass exchanger model for design optimization. *International Journal of Heat and Mass Transfer*. 2011;54(7-8):1344–1351. [155](#)
- [21] Chen D, Li W, Peng H. An experimental study and model validation of a membrane humidifier for PEM fuel cell humidification control. *Journal of power sources*. 2008;180(1):461–467. [155](#)
- [22] Afshari E, Baharlou Houreh N. An analytic model of membrane humidifier for proton exchange membrane fuel cell. *Energy Equipment and Systems*. 2014;2(1):83–94. [155](#), [156](#)
- [23] Yan WM, Li CH, Lee CY, Rashidi S, Li WK. Numerical study on heat and mass transfer performance of the planar membrane-based humidifier for PEMFC. *International Journal of Heat and Mass Transfer*. 2020;157:119918. [156](#)
- [24] Park SK, Choe SY, Choi Sh. Dynamic modeling and analysis of a shell-and-tube type gas-to-gas membrane humidifier for PEM fuel cell applications. *International journal of hydrogen energy*. 2008;33(9):2273–2282. [156](#)

- [25] Sabharwal M, Duelt C, Bhatia D. Two-dimensional modeling of a cross flow plate and frame membrane humidifier for fuel cell applications. *Journal of Membrane Science*. 2012;409:285–301. [158](#)
- [26] Li NF, Huang SM, Liang CH. Entropy and exergy analysis of a hollow fiber membrane humidifier. *Separation and Purification Technology*. 2023;314:123470. [158](#), [159](#)
- [27] Baldinelli G, Rotili A, Narducci R, Di Vona ML, Marrocchi A. Experimental analysis of an innovative organic membrane for air to air enthalpy exchangers. *International Communications in Heat and Mass Transfer*. 2019;108:104332. [159](#)
- [28] Sabek S, Tiss F, Chouikh R, Guizani A. Numerical investigation of heat and mass transfer in partially blocked membrane based heat exchanger: effects of obstacles forms. *Applied Thermal Engineering*. 2018;130:211–220. [159](#)